

https://doi.org/10.1070/QEL16689

Anharmonic Bloch oscillations in a coupler composed of two parallel optical fibre arrays

O.V. Korovay, P.I. Khadzhi, D.A. Markov

Abstract. **The effects of laser beam propagation in a coupler composed of two parallel optical-fibre arrays are studied by the coupled-mode method taking into account the interaction of a given fibre with the nearest neighbours and the linear dependence of the propagation constant on the fibre number. It is shown that, due to the complex structure of each subsystem, the structure of light intensity spatial distribution becomes significantly complicated in the system under study. The occurrence of space limited transverse light diffraction is predicted.**

Keywords: *anharmonic Bloch oscillations, optical fibre array, coupled-mode method.*

1. Introduction

At present, much attention is being paid to the study of linear and nonlinear optical effects in arrays of coupled optical fibres. Such investigations are performed using the coupled-mode method taking into account the interaction of a given fibre with its neighbours, both the nearest and more distant ones. These interactions lead to the occurrence of transverse discrete diffraction in the system of fibres. At high excitation levels, when nonlinear effects become pronounced, light can propagate along fibres in the form of discrete soliton pulses. A number of interesting phenomena arise in these systems: Bloch oscillations [1–13], Zener tunnelling [12–14], dynamic localisation [15–19], etc. Bloch oscillations in an optical fibre array were studied in [1, 8–11] with allowance for the propagation constant correction, linearly changing as a function of the fibre number. Some specific features of light propagation in planar semi-infinite optical fibre arrays with a variable coupling constant between optical fibres were investigated in [12]. A possibility of forming Chebyshev arrays of the first and second kinds, as well as Laguerre, Legendre, Jacobi, and Gegenbauer arrays, was predicted.

Recently, researchers have been greatly interested in the properties of zigzag optical fibre arrays [8–11], where second-order coupling plays an important role in diffraction effects. The results of [1] were generalised in [8–11] to the case of zigzag optical fibre arrays; anharmonic Bloch oscillations in these arrays were studied using the system of coupled-mode equations. An analytical expression for the beam trajectory was found in those studies; it is obtained that it has an oscillating form. The solutions for the beam trajectory make it possible to determine the beam oscillation periods and the coordinates of trajectory turning points.

Apparently, anharmonic Bloch oscillations may also occur in more complex optical objects, e.g., in optical waveguide arrays with an arbitrary law of coupling of an individual fibre with its nearest and more distant neighbours, in blocks of optical fibre arrays, in PT-symmetric systems, etc. As follows from the above brief review of the literature on the subject, the analysis of the specific features of light propagation in complex systems of optical fibres is an urgent problem, interesting from both theoretical and applied points of view. Complex array geometries and the use of new materials, such as graphene, metamaterials, and photonic structures, provide unique possibilities for monitoring and controlling light propagation. Below we present the main results of a theoretical study of the light propagation effects in one of these systems, specifically, in a directed coupler consisting of two parallel optical fibre arrays, with allowance for their coupling with the nearest neighbours and linear dependence of the propagation constant on the fibre number.

2. Basic equations

The starting point of our consideration is the system of equations for the amplitudes of coupled modes of two parallel infinite optical fibre arrays (Fig. 1):

$$\begin{aligned} &\mathrm{i}\frac{\mathrm{d}f_n}{\mathrm{d}z} + \beta n f_n + f_{n-1} + f_{n+1} + (\gamma + \alpha n) g_n = 0, \\ &\mathrm{i}\frac{\mathrm{d}g_n}{\mathrm{d}z} + \beta n g_n + g_{n-1} + g_{n+1} + (\gamma + \alpha n) f_n = 0, \end{aligned} \tag{1}$$

were, for simplicity, the term containing the propagation constant β_0 is excluded by simple exponential transformation; $z = \kappa x$; κ is the coupling constant between a given optical fibre and its nearest neighbours; x is the coordinate along the fibre axis; γ is the coupling constant between arrays; β is an anharmonic correction to the propagation constant β_0 in each array, which determines the phase difference between neighbouring fibres in an array; α is a similar correction, taking into account the coupling anharmonicity between arrays; and f_n and g_n are the normalised field amplitudes of the modes propagating in the nth fibre. System of equations (1) is a generalisation of the corresponding system from [10]. In our case two identical optical fibre arrays interact, thus

O.V. Korovay, D.A. Markov Shevchenko Pridnestrovian State University, 25 October str. 128, MD 3300 Tiraspol, Moldova; e-mail: olesya-korovai@mail.ru
P.I. Khadzhi Institute of Applied Physics, Academy of Sciences of Moldova, Akademicheskaya str. 5g, MD 2028 Chisinau, Moldova

Received 27 March 2018; revision received 29 May 2018
Kvantovaya Elektronika **49** (2) 150–156 (2019)
Translated by Yu.P. Sin'kov

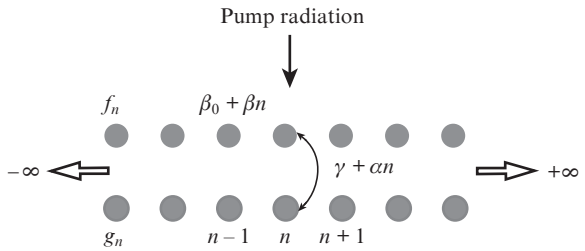

Figure 1. Schematic arrangement of optical fibres in two parallel infinite coupled arrays.

forming a directed coupler. We will assume that a light beam with a field amplitude f_0 is pumped only to the zero fibre of the first array. Then the initial conditions for system (1) can be written as

$$f_n|_{z=0} = f_0\delta_{n0}, \quad g_n|_{z=0} = 0, \tag{2}$$

where δ_{n0} is the Kronecker delta. Having introduced two new functions, $u_n = f_n + g_n$ and $v_n = f_n - g_n$, we derive two independent differential-difference equations from (1) for them,

$$\begin{aligned} &\mathrm{i}\dot{u}_n + (\gamma + \alpha n + \beta n)u_n + u_{n-1} + u_{n+1} = 0, \\ &\mathrm{i}\dot{v}_n - (\gamma + \alpha n - \beta n)v_n + v_{n-1} + v_{n+1} = 0, \end{aligned} \tag{3}$$

with the initial conditions

$$u_n|_{z=0} = v_n|_{z=0} = f_0\delta_{n0}. \tag{4}$$

Let us first consider the solution of the first equation from (3) for the function $u_n(z)$. Having assumed that

$$u_n(z) = F_n(z)\exp[\mathrm{i}(\gamma + \alpha n + \beta n)z], \tag{5}$$

we derive the following equation for $F_n(z)$ from (3):

$$\mathrm{i}\frac{\mathrm{d}F_n}{\mathrm{d}z} + F_{n-1}(z)\exp[-\mathrm{i}(\alpha+\beta)z] + F_{n+1}(z)\exp[\mathrm{i}(\alpha+\beta)z] = 0, \tag{6}$$

with the initial condition $F_n(z)|_{z=0} = f_0\delta_{n0}$. Then we apply a Fourier transform to the function $F_n(z)$:

$$F_n(z) = \frac{1}{2\pi}\int_{-\pi}^{\pi} F(\theta, z)\exp(-\mathrm{i}n\theta)\,\mathrm{d}\theta. \tag{7}$$

Substituting (7) into (6), we obtain a first-order differential equation for the Fourier transform $F(\theta, z)$,

$$\frac{\mathrm{d}F(\theta,z)}{F(\theta,z)} = 2\mathrm{i}\cos[\theta - (\alpha+\beta)z]\mathrm{d}z, \tag{8}$$

whose solution, with allowance for the initial conditions, has the form

$$F(\theta, z) = \exp\left[\frac{4\mathrm{i}}{\alpha+\beta}\sin\left(\frac{\alpha+\beta}{2}z\right)\cos\left(\theta - \frac{\alpha+\beta}{2}z\right)\right]. \tag{9}$$

Substituting (9) into (7) and using the well-known relation [20, 21]

$$\exp(\mathrm{i}z\cos\varphi) = \sum_{k=-\infty}^{+\infty}\mathrm{i}^k J_k(z)\exp(\mathrm{i}k\varphi), \tag{10}$$

where $J_k(z)$ is the kth-order Bessel function, we find the solution for the function $F_n(z)$:

$$F_n(z) = \mathrm{i}^n J_n\left(\frac{4}{\alpha+\beta}\sin\left(\frac{\alpha+\beta}{2}z\right)\right)\exp\left(-\mathrm{i}n\frac{\alpha+\beta}{2}z\right). \tag{11}$$

Then the function $u_n(z)$, in correspondence with (5), can be written as

$$u_n(z) = \mathrm{i}^n J_n\left(\frac{4}{\alpha+\beta}\sin\left(\frac{\alpha+\beta}{2}z\right)\right)\exp\left[\mathrm{i}\left(\gamma + n\frac{\alpha+\beta}{2}\right)z\right]. \tag{12}$$

Similarly, using the second equation from (3), one can obtain a solution for $v_n(z)$:

$$v_n(z) = \mathrm{i}^n J_n\left(\frac{4}{\alpha-\beta}\sin\left(\frac{\alpha-\beta}{2}z\right)\right)\exp\left[-\mathrm{i}\left(\gamma + n\frac{\alpha-\beta}{2}\right)z\right]. \tag{13}$$

Then the final solutions to initial Eqns (1) for the functions $f_n(z)$ and $g_n(z)$ take the form

$$\begin{aligned} f_n(z) = \frac{1}{2}\mathrm{i}^n\Bigg\{&J_n\left(\frac{4}{\alpha+\beta}\sin\left(\frac{\alpha+\beta}{2}z\right)\right)\exp\left[\mathrm{i}\left(\gamma + n\frac{\alpha+\beta}{2}\right)z\right] \\ &+ J_n\left(\frac{4}{\alpha-\beta}\sin\left(\frac{\alpha-\beta}{2}z\right)\right)\exp\left[-\mathrm{i}\left(\gamma + n\frac{\alpha-\beta}{2}\right)z\right]\Bigg\}, \end{aligned} \tag{14}$$

$$\begin{aligned} g_n(z) = \frac{1}{2}\mathrm{i}^n\Bigg\{&J_n\left(\frac{4}{\alpha+\beta}\sin\left(\frac{\alpha+\beta}{2}z\right)\right)\exp\left[\mathrm{i}\left(\gamma + n\frac{\alpha+\beta}{2}\right)z\right] \\ &- J_n\left(\frac{4}{\alpha-\beta}\sin\left(\frac{\alpha-\beta}{2}z\right)\right)\exp\left[-\mathrm{i}\left(\gamma + n\frac{\alpha-\beta}{2}\right)z\right]\Bigg\}. \end{aligned} \tag{15}$$

and the propagating-wave intensities $|f_n(z)|^2$ and $|g_n(z)|^2$ are described by the expressions

$$\begin{aligned} |f_n|^2 = \frac{1}{4}\Bigg\{&J_n^2\left(\frac{4}{\alpha+\beta}\sin\left(\frac{\alpha+\beta}{2}z\right)\right) + J_n^2\left(\frac{4}{\alpha-\beta}\sin\left(\frac{\alpha-\beta}{2}z\right)\right) \\ &+ 2J_n\left(\frac{4}{\alpha+\beta}\sin\left(\frac{\alpha+\beta}{2}z\right)\right)J_n\left(\frac{4}{\alpha-\beta}\sin\left(\frac{\alpha-\beta}{2}z\right)\right) \\ &\times\cos[(2\gamma + n\alpha)z]\Bigg\}, \\ |g_n|^2 = \frac{1}{4}\Bigg\{&J_n^2\left(\frac{4}{\alpha+\beta}\sin\left(\frac{\alpha+\beta}{2}z\right)\right) + J_n^2\left(\frac{4}{\alpha-\beta}\sin\left(\frac{\alpha-\beta}{2}z\right)\right) \\ &- 2J_n\left(\frac{4}{\alpha+\beta}\sin\left(\frac{\alpha+\beta}{2}z\right)\right)J_n\left(\frac{4}{\alpha-\beta}\sin\left(\frac{\alpha-\beta}{2}z\right)\right) \\ &\times\cos[(2\gamma + n\alpha)z]\Bigg\}. \end{aligned} \tag{16}$$

Using (16) and the relation

$$\sum_{n=-\infty}^{+\infty} J_n^2(x) = 1$$

from [22, 23], one can easily show that

$$\sum_{n=-\infty}^{+\infty}(|f_n|^2 + |g_n|^2) = f_0^2. \tag{17}$$

This relation is the energy conservation law in the system: the sum of the energies over all optical fibres in both arrays is retained at any point, independent of the coordinate z, and is equal to the energy supplied to the zero-fibre end face ($z = 0$).

Assuming that $\gamma = 0$ and $\alpha = 0$ in (14) and (15) (i.e., there is no coupling between the first and second arrays), we arrive at the solution for an individual array [1]:

$$|f_n(z)|^2 = J_n^2\left(\frac{4}{\beta}\sin\left(\frac{\beta}{2}z\right)\right), \quad |g(z)|^2 = 0. \tag{18}$$

In another particular case, where only $\alpha = 0$ (there is no coupling anharmonicity between the arrays, but anharmonicity is retained for each array), the expressions for the radiation intensities in fibres have the form

$$\begin{pmatrix}|f_n|^2\\|g_n|^2\end{pmatrix} = J_n^2\left(\frac{4}{\beta}\sin\left(\frac{\beta}{2}z\right)\right)\begin{pmatrix}\cos^2(\gamma z)\\\sin^2(\gamma z)\end{pmatrix}. \tag{19}$$

If $\beta = 0$ (there is no coupling anharmonicity between fibres in an array), we arrive at the following expressions for the radiation intensities:

$$\begin{pmatrix}|f_n|^2\\|g_n|^2\end{pmatrix} = J_n^2\left(\frac{4}{\alpha}\sin\left(\frac{\alpha}{2}z\right)\right)\begin{pmatrix}\cos^2\left[\left(\gamma+\frac{\alpha n}{2}\right)z\right]\\\sin^2\left[\left(\gamma+\frac{\alpha n}{2}\right)z\right]\end{pmatrix}. \tag{20}$$

Finally, if $\alpha = \beta$ (the coupling anharmonicity between the arrays and within each array is the same), we have the expressions:

$$\begin{pmatrix}|f_n|^2\\|g_n|^2\end{pmatrix} = \frac{1}{4}\left\{J_n\left(\frac{2}{\alpha}\sin(\alpha z)\right) + J_n(2z) + 2J_n\left(\frac{2}{\alpha}\sin(\alpha z)\right)J_n(2z)\begin{pmatrix}\cos[(2\gamma+\alpha n)z]\\\sin[(2\gamma+\alpha n)z]\end{pmatrix}\right\}^2. \tag{21}$$

3. Results and discussion

Let us first consider the simplest case, where coupling with neighbouring-array fibres is absent ($\gamma = \alpha = 0$). Under these conditions, pumping is performed only into the end face of the first-array zero fibre. In this case, radiation is not supplied to the second-array fibres; therefore, $|g_n(z)|^2 = 0$. Light propagates only through the first-array fibres. As follows from (18), the intensity of light propagating through the nth fibre depends on the coordinate z and the fibre number n. The spatial distribution of the nth-fibre field intensity periodically changes with an increase in the coordinate z along the fibre axis (Fig. 2).

Figure 3 shows the first period of the spatial distribution of light intensity in array fibres. In the zero (pumped) fibre, the light intensity is equal to f_0^2 at the points $z_k = k\pi/\beta$ ($k = 0, 2, 4, \ldots$) (Fig. 2), i.e., the spatial intensity distribution in a given fibre is periodically repeated with a spatial period $T = 2\pi/\beta$. Within one period, the light intensity in the fibre oscillates, so that the oscillation envelope first slowly decreases from the point $z_0 = 0$ to the point with a coordinate $z_1 = \pi/\beta$, after which it monotonically increases to the end of the period, $z_2 = T = 2\pi/\beta$ (Fig. 3). The reason is that, due to the coupling between neighbouring fibres, light is transferred from the pumped optical fibre to its nearest neighbours, then from these fibres to the next ones, etc.

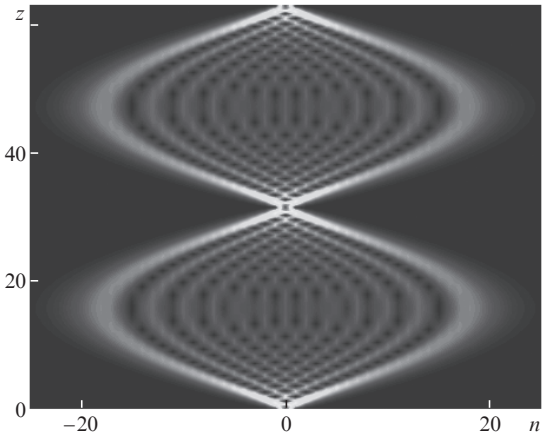

Figure 2. Spatial distribution of light intensity in the first array as a function of coordinate z at $\gamma = \alpha = 0$ and $\beta = 0.01$.

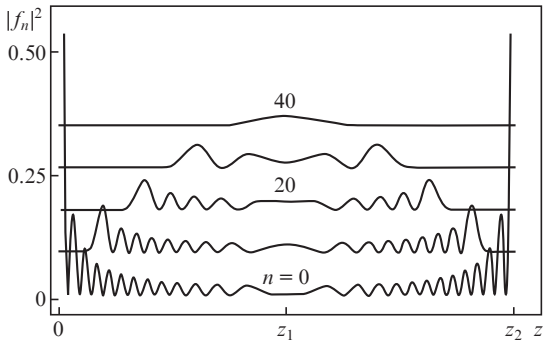

Figure 3. Spatial distributions of field intensity for a series of optical fibres with different numbers n in an array within the first period. Zeros of the functions $|f_n|^2$ are shifted for clarity.

This light propagation regime can be considered as diffusion in the direction perpendicular to the fibre axis. The intensity distribution is periodic due to the periodicity of the function $\sin(\beta z/2)$ in the argument of the Bessel function. The sine value first increases with an increase in z from zero to unity and then decreases from unity to zero; the Bessel function oscillates during the first half-period, with a monotonically decreasing oscillation amplitude. During the second half-period, the Bessel function repeats the evolution of the first half-period but in reverse order. At large n values, the Bessel function remains zero for a long time, and only at large values of the argument (i.e., large z values) it rapidly increases; possibly, makes few oscillations; and them changes again in reverse order. It can be seen in Fig. 3 that the amplitudes of light intensity oscillations in the middle of the period are smaller than in the beginning and end of the period. If the $4/\beta$ value is smaller than the amplitude of the first maximum of the nth-order Bessel function, there are practically no observable disturbances in the n-th fibre, and specifically this fact determines the maximum transverse size of the region of disturbed array fibres.

The spatial intensity distribution in other (unpumped) fibres is also a sequence of maxima, separated by field zeros.

The coordinates z_{nk} of zero intensity values are given by the expression

$$z_{nk} = \frac{2}{\beta}\left[\arcsin\left(\frac{\beta}{4} j_{nk}\right) + k\pi\right],$$

where j_{nk} is the kth zero of nth-order Bessel function.

It follows from expressions (18) and Fig. 4 that the characteristic period of changes in the spatial field distribution tends to infinity at $\beta \to 0$. This means that, at $\beta \to 0$, the disturbed array region is located between straight lines that are symmetric with respect to the pumped optical fibre, because $|f_{-n}(z)|^2 = |f_n(z)|^2$ (Fig. 4). At $\beta \neq 0$ the largest distance between the zero fibre and the fibre reached by light is determined by the expression $z = z_1 = \pi/\beta$. Thus, the maximum transverse size of the region of disturbed fibres monotonically decreases with an increase in β (Fig. 4).

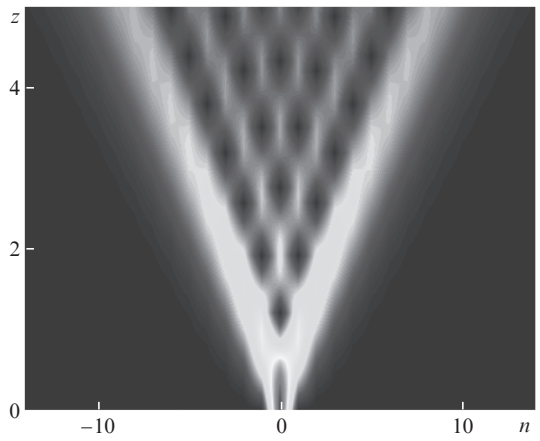

Figure 4. Spatial distribution of light intensity in the first array in dependence of coordinate z at $\gamma = \alpha = 0$ and $\beta = 0.2$.

Let us now consider the spatial distribution of light intensity in the case of only linear coupling ($\gamma \neq 0$, $\alpha = 0$) between the arrays. It follows from expressions (19) that the functions $|f_n(z)|^2$ and $|g_n(z)|^2$ are characterised by two spatial periods (Fig. 5). One of these periods is due, as in the previous case, to the change in the Bessel function argument $\sin(\beta z/2)$, while the other period is caused by the factor $\cos^2(\gamma z)$ for the function $|f_n(z)|^2$ or the factor $\sin^2(\gamma z)$ for the function $|g_n(z)|^2$. These factors determine the transfer rate for light with a period $T_1 = \pi/\gamma$, which is characteristic of a coupler consisting of two parallel optical fibres with a coupling constant γ. Therefore, the spatial distribution of light intensity in the first array is the same as the distribution obtained for $f^2(z) = J_n^2((4/\beta)\sin(\beta z/2))$ at $\gamma = 0$ (Fig. 2), but additionally modulated by the function $\cos^2(\gamma z)$ (Fig. 5a). Therefore, the spatial light intensity distribution in the second array is given by the function $|g_n(z)|^2$ at $\gamma = 0$, modulated by the function $\sin^2(\gamma z)$ at $\beta = \gamma$ (Fig. 5b).

The positions of zeros and extrema of the factors $\cos^2(\gamma z)$ and $\sin^2(\gamma z)$, which determine the light transfer rate between the arrays, are independent of the fibre number n. The spatial distribution of light intensity in the arrays depends on the intensity maxima positions (determined by the Bessel function value $z = z_1 = \pi/\beta$), which coincide with the positions of minima $z = z_2 = \pi/2\gamma$ of the function $\sin^2(\gamma z)$, $z_1 = z_2$, at $\beta = 2\gamma$ (Fig. 5). Dark transverse bands correspond to zero field values in fibres. The centres of these dark bands are located at the points $z_k = (k + 1/2)\pi/\gamma$ in the first array and at the points $z_k = k\pi/\gamma$ in the second array.

The spatial intensity distribution depends strongly on the relationship between the interaction constants β and γ. An analysis of expression (19) shows that the distribution of light intensity maxima in the arrays changes significantly in comparison with that reported in Fig. 2, depending on the relation between β and 2γ. At $\beta < 2\gamma$, the light intensity maxima in the first array are located, as previously, at the distribution nodes (Fig. 6a), whereas the light intensity maxima in the second array are concentrated in extreme excited fibres (Fig. 6), which is indicative of almost complete light transfer between the arrays. At $\beta > 2\gamma$, the positions of intensity distribution maxima in both arrays change. The light intensity is maximal in the zero optical fibre of the first array (Fig. 7a). At a half-period distance, the intensity maximum is transferred to the zero optical fibre of the second array (Fig. 7b). The excited region of the arrays narrows in the transverse direction in comparison with that shown in Fig. 6 because of the light diffusion. At $\beta \gg 2\gamma$, the excited region sharply narrows in the transverse direction, practically to a single fibre (Fig. 8). If $\beta = 0$, the spatial intensity distribution $|f_n(z)|^2$ is a set of max-

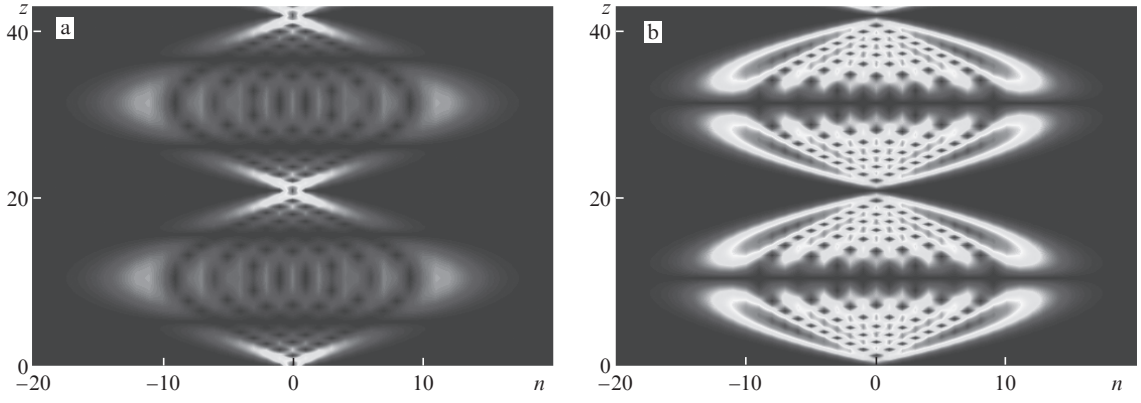

Figure 5. Spatial distributions of light intensity in the (a) first and (b) second arrays as a function of coordinate z at $\alpha = 0$ and $\gamma = \beta = 0.3$.

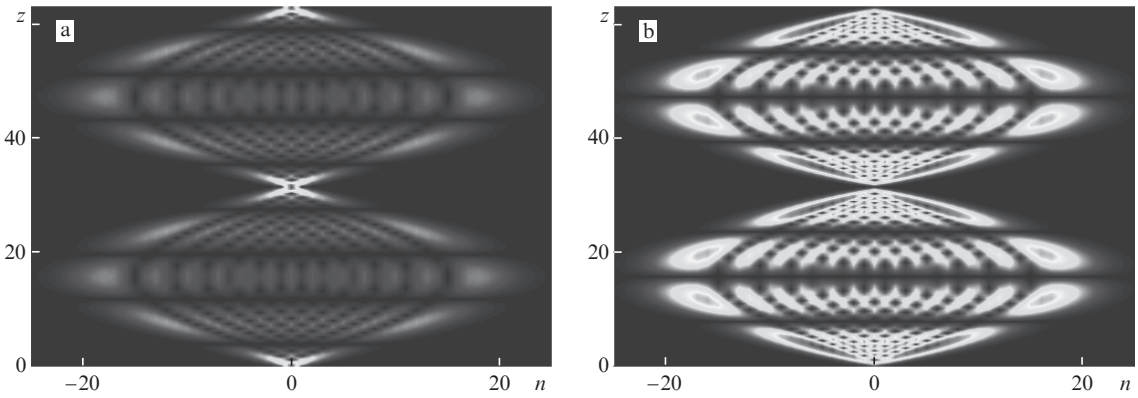

Figure 6. The same as in Fig. 5 but at $\alpha = 0$, $\gamma = 0.4$, and $\beta = 0.2$.

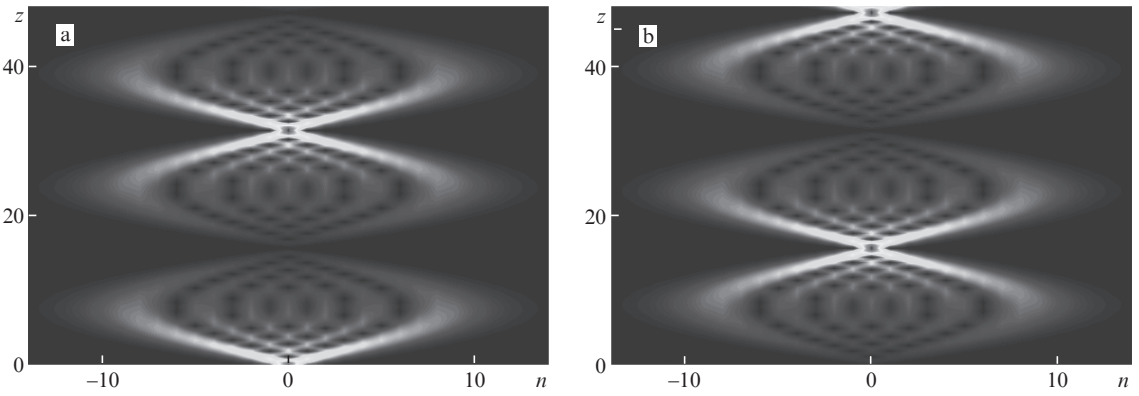

Figure 7. The same as in Fig. 5 but at $\alpha = 0$, $\gamma = 0.1$, and $\beta = 0.4$.

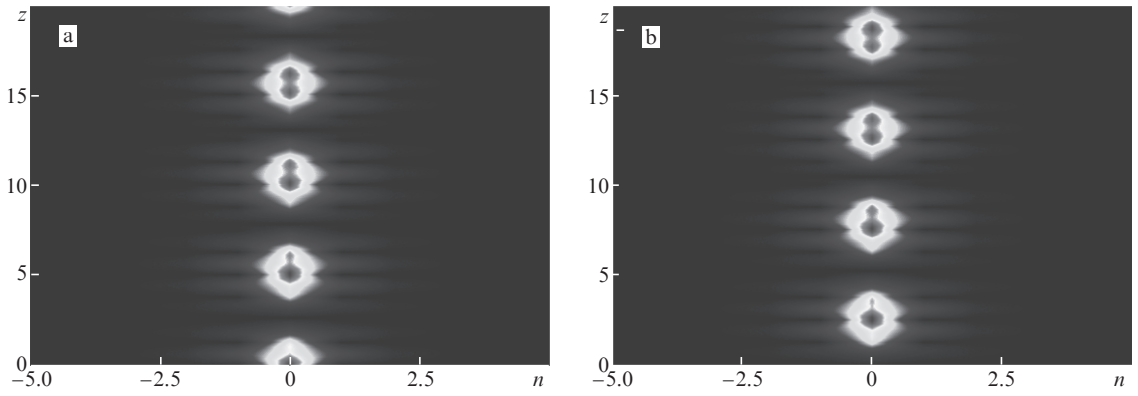

Figure 8. The same as in Fig. 5 but at $\alpha = 0$, $\gamma = 0.6$, and $\beta = 5$.

ima and minima (zeros) with a period $T_1 = \pi/\gamma$, located between two straight lines containing the first maxima of the Bessel function $J_n^2(2z)$ (Fig. 9).

If there is no coupling anharmonicity between fibres in an array ($\beta = 0$) and $\alpha \neq \gamma \neq 0$, the spatial distribution of light intensity remains periodic. The complete-transfer period between the arrays is $T = 2\pi/\alpha$. Spatial oscillations of intensity distribution occur within this period. The positions of intensity maxima and minima in both the first and second arrays are asymmetric with respect to the zero fibre (Fig. 10). The factor $\sin^2[(\gamma + \alpha n/2)z]$ in (20) determines the existence of unexcited fibre with a number $n = -2\gamma/\alpha$ in the second array (Fig. 10b).

Finally, the spatial distributions of light intensity in the first and second optical fibre arrays are presented in Figs 11–13. One can see a complex superposition of oscillations with several periods, the number of which depends on the parameters of the system.

4. Conclusions

The spatial intensity distribution for light propagating in two coupled parallel optical fibre arrays was studied by the coupled-mode method with allowance for the coupling of fibres with their nearest neighbours and the linear dependence of the propagation constant on the fibre number. It was shown

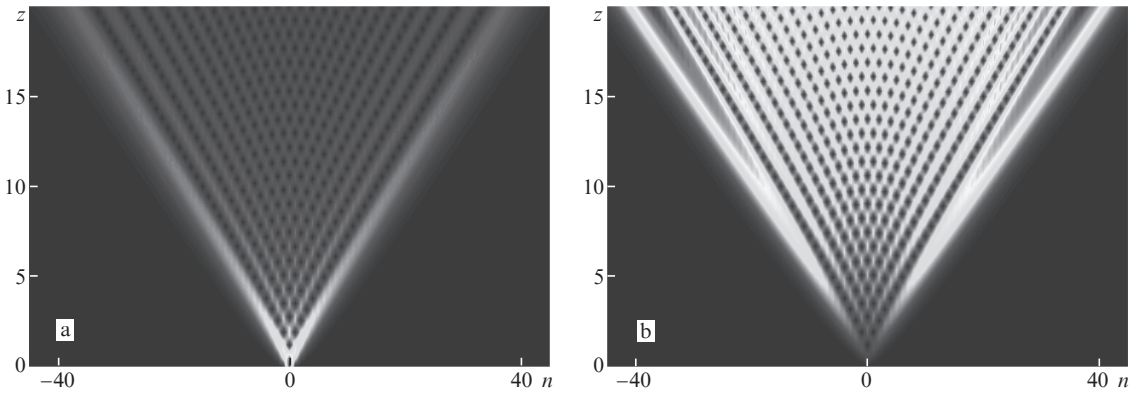

Figure 9. The same as in Fig. 5 but at $\alpha = \beta = 0$ and $\gamma = 0.01$.

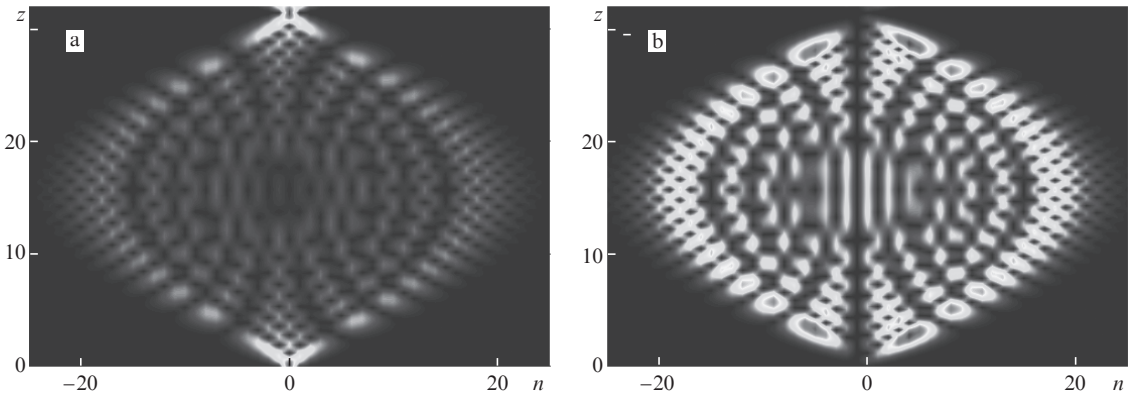

Figure 10. The same as in Fig. 5 but at $\alpha = 0.2$, $\gamma = 0.1$, and $\beta = 0$.

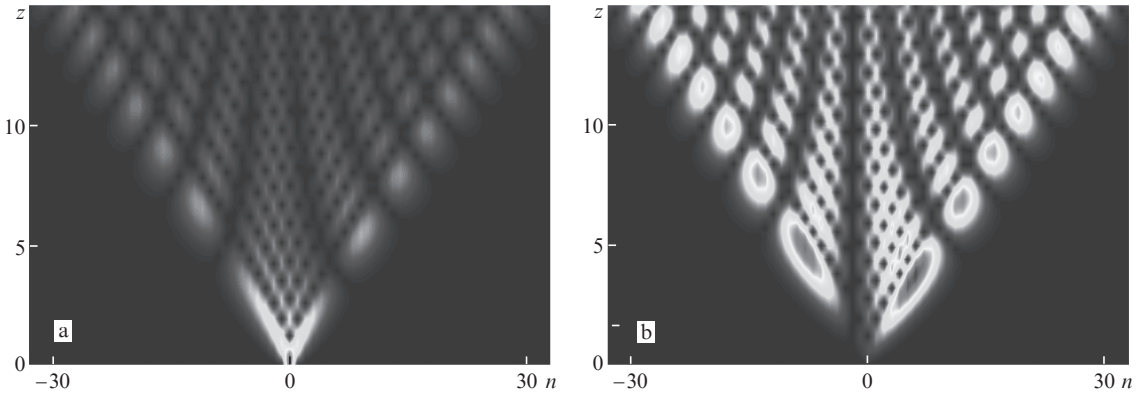

Figure 11. The same as in Fig. 5 but at $\alpha = \gamma = \beta = 0.1$.

that the distribution of light intensity is a periodic function of coordinate. The dependences of fibre-to-fibre light transfer periods on the system parameters were found. It was established that space limited transverse diffraction of light occurs in the system under consideration. The results of this work may be used to design new quantum electronics devices for light propagation control.

References

1. Peschel U., Pertsch T., Lederer F. *Opt. Lett*., **23**, 1701 (1998).
2. Pertsch T., Dannberg P., Elflein W., Bräuer A., Lederer F. *Phys. Rev. Lett*., **83**, 4752 (1999).
3. Morandotti R., Peschel U., Aitchison J.S., Eisenberg H.S., Silberberg Y. *Phys. Rev. Lett*., **83**, 4756 (1999).
4. Pertsch T., Zentgraf T., Peschel U., Bräuer A., Lederer F. *Appl. Phys. Lett*., **80**, 3247 (2002).
5. Chiodo N., Valle G.D., Osellame R., Longhi S., Cerullo G., Ramponi R., Laporta P., Morgner U. *Opt. Lett*., **31**, 1651 (2006).
6. Longhi S. *Phys. Rev. B*, **76**, 195119 (2007).
7. Zheng M.J., Xiao J.J., Yu K.W. *Phys. Rev. A*, **81**, 033829 (2010).
8. Gozman M.I., Polishchuk Yu.I., Polishchuk I.Ya. *Opt. Eng*., **53** (7), 071806 (2014).
9. Wang G., Huang J.P., Yu K.W. *Opt. Lett*., **35**, 1908 (2010).

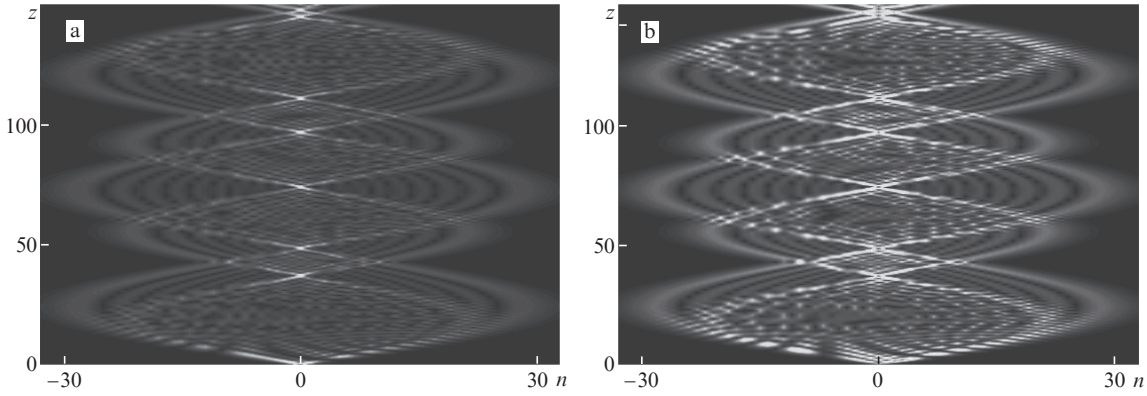

Figure 12. The same as in Fig. 5 but at $\alpha = 0.15$, $\gamma = 0.5$, and $\beta = 0.02$.

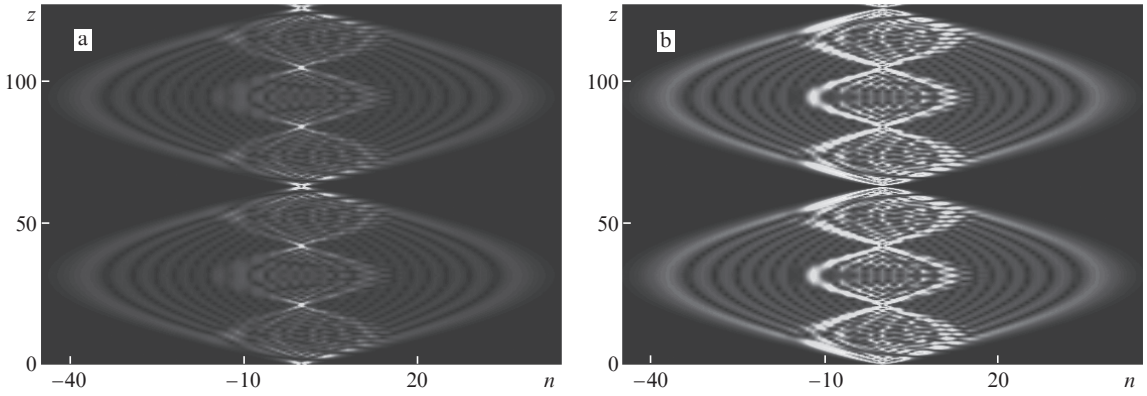

Figure 13. The same as in Fig. 5 but at $\alpha = 0.1$, $\gamma = 0.8$, and $\beta = 0.2$.

10. Gozman M.I., Guseynov A.I., Kagan Yu.M., Pavlov A.I., Polishchuk I.Ya. arXiv:1501.06492 (2015).
11. Korovai O.V., Krukovskii A.P., Khadzhi P.I. *Quantum Electron.*, **48** (1), 37 (2018) [*Kvantovaya Elektron.*, **48** (1), 37 (2018)].
12. Khadzhi P.I., Lyakhomskaya K.D., Orlov O.K. *Quantum Electron.*, **36** (10), 971 (2006) [*Kvantovaya Elektron.*, **36** (10), 971 (2006)].
13. Dreisow F., Wang G., Heinrich M., Keil R., Tünnermann A., Nolte S., Szameit A. *Opt. Lett.*, **36** (2), 3954 (2011).
14. Zheng M.J., Wang G., Yu K.W. *Opt. Lett.*, **35** (23), 3865 (2010).
15. Dreisow F., Szameit A., Heinrich M., Pertsch T., Nolte S., Tünnermann A., Longhi S. *Phys. Rev. Lett.*, **102**, 076802 (2009).
16. Trompeter H., Pertsch T., Lederer F., Michaelis D., Streppel U.. Bräuer A., Peschel U. *Phys. Rev. Lett.*, **96**, 023901 (2006).
17. Schwartz T., Fishman S., Segev M. *Electron. Lett.*, **44** (3), 165 (2008).
18. Lahini Y., Avidan A., Pozzi F., Sorel M., Morandotti R., Chistodoulides D.N., Silberberg Y. *Phys. Rev. Lett.*, **100**, 013906 (2008).
19. Garanovich I.I., Szameit A., Sukhorukov A.A., Pertsch T., Krolikowski W., Nolte S., Neshev D., Tünnermann A., Kivshar Y.S. *Opt. Express*, **15** (15), 9737 (2007).
20. Gradshtein I.S., Ryzhik I.M. *Table of Integrals, Series, and Products* (New York: Academic Press, 1980).
21. Korn G.A., Korn T.M. *Mathematical Handbook for Scientists and Engineers* (New York: McGraw-Hill, 1968; Moscow: Nauka, 1974).
22. Dreisow F., Heinrich M., Szameit A., Döring S., Nolte S., Tünnermann A., Fahr S., Lederer F. *Opt. Express*, **16** (5), 3474 (2008).
23. Salerno M., Konotop V.V., Bludov Y.V. *Phys. Rev. Lett.*, **101**, 30405 (2008).